FluorMODleaf: A new leaf fluorescence emission model based on the PROSPECT model

R. Pedrós [a,b,c], Y. Goulas [b,*], S. Jacquemoud [c], J. Louis [d], I. Moya [b]

[a] Solar Radiation Group, Department of Earth Physics and Thermodynamics, University of Valencia, Spain
[b] Equipe de Fluorescence, Laboratoire de Météorologie Dynamique, Centre National de la Recherche Scientifique, UMR 8359, Palaiseau, France
[c] Equipe de Géophysique Spatiale et Planétaire, Institut de Physique du Globe de Paris et Université Paris Diderot, UMR 7154, Paris, France
[d] Equipe de Biospectroscopie Végétale, Laboratoire Ecologie Systématique et Evolution, UMR 8079, Orsay, France

ARTICLE INFO

ABSTRACT

A new model of chlorophyll *a* fluorescence emission by plant leaves, FluorMODleaf, is presented. It is an extension of PROSPECT, a widely used leaf optical properties model that regards the leaf as a pile of N absorbing and diffusing elementary plates. In FluorMODleaf, fluorescence emission of an infinitesimal layer of thickness dx is integrated over the entire elementary plate. The fluorescence source function is based on the excitation spectrum of diluted isolated thylakoids and on the emission spectra of isolated photosystems, PSI and PSII, which are the main pigment–protein complexes involved in the initial stages of photosynthesis. Scattering within the leaf is produced by multiple reflections within and between elementary plates. The input variables of FluorMODleaf are: the number of elementary plates N, also called leaf structure parameter, the total chlorophyll content C_{ab}, the total carotenoid content C_{cx}, the equivalent water thickness C_w, and the dry matter content C_m (or leaf mass per area), as in the new PROSPECT-5, plus the σ_{II}/σ_I ratio referring to the relative absorption cross section of PSI and PSII, and the fluorescence quantum efficiency of PSI and PSII, τ_I and τ_{II}, that are introduced here as mean fluorescence lifetimes. The model, which considers the reabsorption of emitted light within the leaf, allows good quantitative estimation of both upward and downward apparent spectral fluorescence yield (ASFY) at different excitation wavelengths from 400 nm to 700 nm. It also emphasizes the role of scattering in fluorescence emission by leaves having high chlorophyll content.

© 2009 Elsevier Inc. All rights reserved.

1. Introduction

In the past 30 years, Earth observation from space has demonstrated its ability to monitor changes at a global scale. The complexity of physical, chemical, and biological processes that occur in terrestrial ecosystems requires detailed characterization of the natural environment and assessment of the interactions between soil, vegetation, and atmosphere to understand biosphere functioning (Monteith & Unsworth, 2007). This can be fulfilled by coupling physics-based canopy functioning models with remote sensing data that also require advanced quantitative methods to exploit information of all kinds present in the radiometric signal. Since they are not directly linked to fundamental processes of plant physiology, like photosynthesis, multispectral and/or multiangular reflectance factors measured by present optical sensors only provide partial information on vegetation dynamics, especially on a short timescale. In other words, one cannot monitor photosynthesis using only vegetation reflectance. Chlorophyll fluorescence (ChlF) is known to carry very specific information about leaf light-use efficiency, i.e., plant vitality and biomass productivity. Passive remote sensing techniques like the measurement of solar-induced chlorophyll fluorescence, which is modulated by photosynthetic efficiency, should improve our knowledge of the terrestrial carbon cycle and help us monitoring vegetation health from airborne or spaceborne platforms (Moya et al. 1992; Davidson et al., 2003; Moya & Cerovic, 2004; Grace et al., 2007; Guanter et al., 2007).

Both at leaf and canopy levels, fluorescence emission is an intricate response of environmental and physiological factors. To sort them out and better interpret this signal, the European Space Agency funded the FluorMOD project (ESA contract no. 16365/02/NL/FF) that aimed at developing an integrated top-of-atmosphere vegetation fluorescence model (Miller et al., 2005). A detailed description of light interaction with single vegetation elements, i.e., plant leaves, both at excitation and emission wavelengths, is the first link in the chain that will permit full exploitation of the fluorescence emission signal measured by a remote sensor.

Most fluorescence models have been developed for other applications than plant physiology, like medical diagnosis of human diseases (e.g., Wu et al., 1993; Georgakoudi, 2006; Gupta et al., 2006) or quality color control for the paper industry (e.g., Emmel, 1998, 2000; Emmel & Hersch, 1998) where fluorescence spectroscopy is widely used. In

---

* Corresponding author. Laboratoire de Météorologie Dynamique, Ecole Polytechnique, F91128 Palaiseau Cedex, France.
E-mail address: yves.goulas@lmd.polytechnique.fr (Y. Goulas).

most media, the measured emission spectrum is distorted due to light reabsorption and/or scattering, which makes its interpretation especially difficult. Different theories have emerged that attempt to explain the propagation of light in a turbid medium, including fluorescence emission: radiative transfer equation (Richards-Kortum et al., 1989; Gardner et al., 1996; Emmel & Hersch, 1998), two-flux Kubelka–Munk (KM) theory and four-flux extensions (Allen, 1964; Fukshansky & Kazarinova, 1980; Bonham, 1986; Shakespeare & Shakespeare, 2003), Monte Carlo simulations (Wu et al., 1993; Crilly et al., 1997; Welch et al., 1997), or rigorous analysis of tissue fluorescence based on electromagnetic theory (Panou-Diamandi et al., 1998).

Conversely, there are few leaf fluorescence models in the literature. They are based on different theories of light propagation within a plant leaf. The simplest ones assume an exponential light decay within the blade, which follows Beer's law (Agati et al., 1993; Ounis et al., 2001). The Kubelka–Munk differential equations are preferred by Rosema et al. (1991), Zarco-Tejada et al. (2000), and Ramos and Lagorio (2004) who solve the system analytically by successive approximations or numerically using the adding-doubling technique. Other approaches like Markov chains (Maier, 2000) or Monte Carlo photon transport (Sušila & Nauš, 2007) have also been developed. The main challenge in leaf fluorescence modeling lies in the accurate simulation of light reabsorption and its impact on fluorescence emission. For this purpose, empirical methods have been proposed to correct the fluorescence emission spectrum (Gitelson et al., 1998), but these methods provide results that differ from outputs of physically-based models (Cordon & Lagorio, 2006, 2007a, b). Not many of these simulated fluorescence emission spectra have been actually compared to measurements, most of the time they are expressed in relative units and their spectral resolution is higher than 5 nm. This is inadequate for top-of-atmosphere studies, particularly in the narrow oxygen absorption bands of the solar spectrum that are intensively investigated for passive ChlF emission measurements. Moreover, some of these models definitely calculate the fluorescence spectrum of a leaf but not its reflectance and transmittance, and when these are available, they are seldom validated. In consequence, there is a need for a leaf fluorescence model supported by strong physical assumptions, running with a limited number of input variables, and simulating ChlF with accuracy.

In this paper, we present a new leaf fluorescence model, FluorMODleaf, which is derived from the PROSPECT model. The first section presents the material and methods implemented to measure PSI and PSII excitation spectra. The second one details the physics of scattering, absorption and fluorescence emission within the model, as well as the fluorescence source function, i.e., the model of fluorescence emission at the chloroplast level. In the third section, a sensitivity analysis of the model and a comparison of its outputs with experimental measurements are presented. The conclusion goes back over the potentials and limits of FluorMODleaf.

2. Materials and methods

Intact chloroplasts were isolated from spinach (*Spinacia oleracea* L.) as described in Laasch (1987) and then osmotically shocked. The thylakoids obtained this way at a concentration of 1.6 mg Chl ml^{-1} were diluted for fluorescence measurements. PSII and PSI samples were prepared according to Berthold et al. (1981) and Mullet et al. (1980), respectively. In order to avoid reabsorption artifacts, all fluorescence emission and excitation spectra were measured in a 1 cm path length quartz cuvette and diluted until they remained unchanged (final chlorophyll concentration of about 1–2 µg ml^{-1}). Fluorescence excitation spectra of thylakoids, PSI and PSII suspensions were obtained with the Cary Eclipse fluorescence spectrophotometer (Varian Inc., U.S.A.) by varying the excitation wavelength at a fixed emission wavelength of 740 nm. The spectral resolution is 1 nm. To correct the shape of the excitation spectra, the intensity $S(\lambda)$ of the excitation beam generated

by the xenon flash-lamp of the spectrometer was measured using a calibrated photodiode (S1337-1010BQ, Hamamatsu Photonics, Japan). Corrected excitation spectra were obtained by dividing the experimental spectrum by $S(\lambda)$ expressed in quantum units.

3. Description of the model

FluorMODleaf is the name given to the leaf fluorescence model that we designed to predict the reflectance, transmittance, upward and downward ChlF emission of a green leaf supposing that it is isolateral. It is based on PROSPECT, a radiative transfer code that pioneered the computation of the directional–hemispherical reflectance (DHR) and transmittance (DHT) of various plant leaves (monocots and dicots) over the solar spectrum, and which is now widely used in the remote sensing community (Jacquemoud & Baret, 1990). The model mimics the leaf as a stack of several absorbing plates with rough surfaces giving rise to isotropic diffusion (Benford, 1923; Allen et al., 1970). The main advantage of PROSPECT is that *i*) it has few input variables, *ii*) absorption and scattering of light are well separated, *iii*) model inversion can be easily performed for calibration or validation purposes, and *iv*) the input variables can be either measured or estimated.

PROSPECT-5, the very last version of the model recently published by Feret et al. (2008), needs five input variables to calculate the DHR and DHT from 400 nm to 2500 nm at a spectral resolution of 1 nm: the leaf structure parameter N that represents the number of compact layers specifying the amount of cell wall-air space interfaces within the mesophyll, the chlorophyll $a + b$ content C_{ab} (µg cm^{-2}), the total carotenoid content C_{cx} (µg cm^{-2}), the equivalent water thickness C_w (g cm^{-2} or cm), and the dry matter content C_m also called leaf mass per area (g cm^{-2}). Like in PROSPECT, the FluorMODleaf model considers homogeneous absorbing plates with rough surfaces, except that the intra-plate medium is fluorescent. We introduce F_u and F_d as the upward and downward fluorescence coefficients of the plate, respectively, and the observed fluorescence fluxes are $F_u^{i_0}$ and $F_d^{i_0}$, respectively, when the leaf is illuminated by the excitation flux i_0.

3.1. Fluorescence of a single plate

3.1.1. Computation of absorbed flux in an elementary layer

Consider a single plate illuminated by incident light i_0 that is a function of wavelength and that can be either a direct flux, a diffuse flux, or a mixture (Fig. 1). As the plate surface is rough, all fluxes reflected or transmitted at the interface of the medium are isotropic. In Fig. 1, these fluxes are designated i_1, j_1, i_3 and j_3. We define an infinitesimal horizontal layer $L(x)$ inside the plate, located at depth x, where x refers to the distance from the top of the plate. The layer $L(x)$ receives the flux $i(x)$ traveling downward from the top of the plate ($x = 0$) and the flux $j(x)$ traveling upward from the bottom ($x = 1$). The fluorescence emission $df(\lambda_{ex}, \lambda_{em}, x)$ at depth x is proportional to the amount of photons absorbed by the infinitesimal layer $L(x)$ and can be written as:

$$df(\lambda_{ex}, \lambda_{em}, x) = \phi(\lambda_{ex}, \lambda_{em})da(\lambda_{ex}, x) \tag{1}$$

where λ_{ex} and λ_{em} are the excitation and emission wavelengths, respectively, $\phi(\lambda_{ex}, \lambda_{em})$ is a source function, and $da(\lambda_{ex}, x)$ is the absorbed flux. The source function $\phi(\lambda_{ex}, \lambda_{em})$ is the spectral fluorescence yield (SFY) of the elementary layer, which can be defined as the probability that one photon absorbed by the medium at λ_{ex} be emitted at λ_{em}. The absorbed flux $da(\lambda_{ex}, x)$ is related to flux variations through the layer $L(x)$, therefore it can be calculated by deriving the propagating fluxes $i(x)$ and $j(x)$ with respect to x:

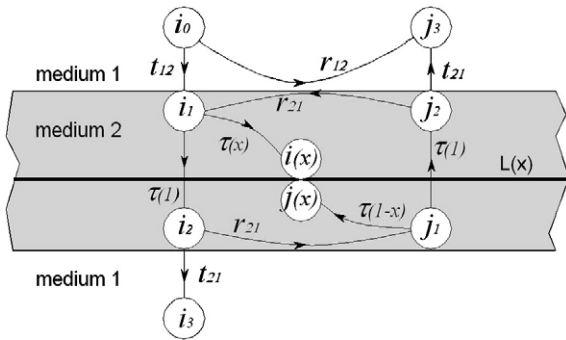$$da(x) = (i(x) - i(x + dx)) + (j(x + dx) - j(x)) = \left(-\frac{di}{dx}(x) + \frac{dj}{dx}(x) \right)dx. \tag{2}$$

Fig. 1. Flux network in a semi-transparent plate made of an absorbing medium with rough surfaces. i_0, i_1, i_2, i_3 and $i(x)$ are the downward fluxes. j_0, j_1, j_2 and $j(x)$ are the upward fluxes. i_1, i_2, j_1 and j_2 are the internal fluxes close to the interface. $i(x)$ and $j(x)$ are incident fluxes on an infinitesimal layer $L(x)$. t_{12} (or t_{21}) and r_{12} (or r_{21}) are the transmittance and reflectance of the interface from medium 1 to 2 (or from 2 to 1). $\tau(x)$ is the transmittance of the inner medium for an isotropic light traveling through a section of thickness x.

We propose hereafter to use graphs to represent the internal fluxes within the plate. This graphical method can be applied to any algebraic problem that is intended to compute fluxes, and the appropriate system of equations is intuitively set up: the nodes represent the fluxes and the arrows stand for the physical processes through which one flux is linked with another. As an example, Fig. 1 shows all the fluxes and their interconnections inside a single plate illuminated by an incident radiation i_0. The infinitesimal layer $L(x)$ is also depicted. The flux i_0 is split in two fluxes, i_1 and j_3: the branch from i_0 to i_1 represents the light transmitted through the interface between the air (medium 1) and the plate (medium 2) with a transmissivity (or transmission coefficient) t_{12}. The contribution of this branch to i_1 is then $t_{12}i_0$. The branch connecting i_0 to j_3 corresponds to the partial reflection at the interface between media 1 and 2, with a reflectivity (or reflection coefficient) r_{12}. When several branches converge on a given node, the corresponding flux is obtained by summing all the incoming fluxes attached to them. For example, i_1 is calculated by adding the contributions of i_0 and j_2:

$$i_1 = t_{12}i_0 + r_{21}j_2. \tag{3}$$

Similar rules apply to all fluxes of the network depicted in Fig. 1. This leads to the following system of linear equations:

$$\begin{array}{ll} i_1 = t_{12}i_0 + r_{21}j_2 & j_1 = r_{21}i_2 \\ i_2 = \tau(1)i_1 & j_2 = \tau(1)j_1 \\ i_3 = t_{21}i_2 & j_3 = t_{21}j_2 + r_{12}i_0 \\ i(x) = \tau(x)i_1 & j(x) = \tau(1-x)j_1 \end{array} \tag{4}$$

where r_{12} and t_{12} have been defined earlier, and r_{21} and t_{21} are the reflectivity and transmissivity at the interface separating medium 2 from medium 1. The reflectivity r_{12} is calculated from the Fresnel equations as in PROSPECT (Jacquemoud & Baret, 1990) and t_{12} can be easily deduced *via* the relation $t_{12} = 1 - r_{12}$ when no absorption occurs at the interface. Remembering that $t_{21} = t_{12}/n^2$ avoids unnecessary calculations. The coefficient $\tau(x)$ is the transmissivity of a layer of the inner medium for isotropic radiation traveling from the surface to a level x inside the plate. It can be obtained by integration of Beer's law over the hemisphere (for details, see Miller et al., 2005).

$$\tau(x) = \frac{\int_0^{2\pi} d\varphi \int_0^{\pi/2} \tau(\theta, x)\cos\theta\sin\theta d\theta}{\int_0^{2\pi} d\varphi \int_0^{\pi/2} \cos\theta\sin\theta d\theta} = (1-kx)\exp(-kx) + k^2x^2\Gamma(0, kx) \tag{5}$$

where θ and φ are the zenith and azimuth angles of the incident flux, k is the absorption coefficient of the inner medium and $\Gamma(0, kx)$ is the

"upper" incomplete gamma function. By solving the system of linear Eq. (4), we get the expressions of $i(x)$ and $j(x)$:

$$i(x) = \frac{i_0 t_{12}\tau(x)}{1 - r_{21}^2\tau(1)^2} \tag{6}$$

$$j(x) = \frac{i_0 t_{12}r_{21}\tau(1)\tau(1-x)}{1 - r_{21}^2\tau(1)^2}. \tag{7}$$

Finally, $\frac{di}{dx}(x)$ and $\frac{dj}{dx}(x)$ can be deduced by derivation of Eqs. (6) and (7) with respect to x, assuming that the first derivative of $\tau(x)$ is expressed by:

$$\frac{d\tau}{dx}(x) = 2k^2x\Gamma(0, kx) - 2k\exp(-kx). \tag{8}$$

3.1.2.. Computation of the fluorescence of a single plate

The combination of Eqs. (1), (2), (5)–(7) yields the expression of the fluorescence emission of the infinitesimal layer $L(x)$:

$$df(x) = \phi(\lambda_{em}, \lambda_{ex})\frac{i_0 t_{12}\left(r_{21}\tau(1)\frac{d\tau}{dx}(1-x) - \frac{d\tau}{dx}(x)\right)}{1 - r_{21}^2\tau(1)^2}. \tag{9}$$

To calculate the fluorescence emission of the whole plate, we first have to evaluate the reabsorption of the emitted flux by the inner medium, taking into account internal reflections on the interfaces, and then to integrate the result over the whole plate for x varying between 0 and 1. Once again, the problem can be approached using a network of emitted fluxes to set up the simultaneous equations describing fluorescence reabsorption (Fig. 2):

$$\begin{cases} df_u = t_{f21}df_{u1} \\ df_{u1} = \frac{1}{2}\tau_f(x)df(x) + \tau_f(1)df_{u2} \\ df_{u2} = r_{f21}df_{d2} \\ df_{d1} = r_{f21}df_{u1} \\ df_{d2} = \frac{1}{2}\tau_f(1-x)df(x) + \tau_f(1)df_{d1} \\ df_d = t_{f21}df_{d2} \end{cases} \tag{10}$$

where the subscript f indicates that the fluorescence emission wavelength λ_{em} is involved. Since fluorescence is an isotropic light source, emitted photons are equally distributed between the upward
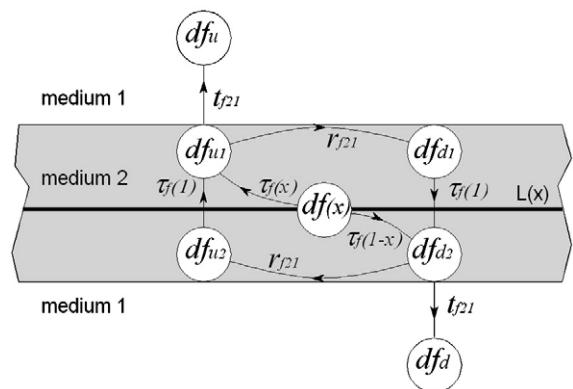

Fig. 2. Flux network of fluorescence emission of the elementary layer $L(x)$ at depth x.

and downward directions and the transmission function $\tau_f(x)$ is simply obtained by replacing k with k_f in $\tau(x)$ (Eq. (5)). The solution of Eq. (10) gives the infinitesimal upward and downward fluorescence fluxes df_u and df_d:

$$\begin{cases} df_u = \dfrac{t_{f21}df(x)(r_{f21}\tau_f(1)\tau_f(1-x) + \tau_f(x))}{2(1-r_{f21}^2\tau_f(1)^2)} \\ df_d = \dfrac{t_{f21}df(x)(\tau_f(1-x) + r_{f21}\tau_f(1)\tau_f(x))}{2(1-r_{f21}^2\tau_f(1)^2)} \end{cases} \tag{11}$$

The upward and downward fluorescence signals $F_u(1)$ and $F_d(1)$ of the whole plate are then obtained as the integral of df_u and df_d from $x = 0$ to $x = 1$:

$$F_u(1) = \int_0^1 df_u \quad \text{and} \quad F_d(1) = \int_0^1 df_d. \tag{12}$$

These expressions cannot be integrated analytically so we did it numerically for a range of k and k_f values in order to build a look-up table and speed up the computation.

3.2. Fluorescence of N plates

Consider now a stack of N uniform fluorescent plates illuminated by an anisotropic incident light beam of intensity i_0, inscribed in a cone defined by its half angle α. The output variables $R_\alpha(N)$ and $T_\alpha(N)$ are the reflectance and the transmittance of this system at the excitation wavelength λ_{ex}. The subscript α is removed when light is isotropic ($\alpha = 90°$). In a similar way, we can define $F_u(N)$ and $F_d(N)$ the upward and downward apparent fluorescence yields of N plates at the emission wavelength λ_{em}. If we add a new plate at the bottom of the stack, the reflectance and transmittance become $R_\alpha(N+1)$ and $T_\alpha(N+1)$ and the upward and downward fluorescence yields $F_u(N+1)$ and $F_d(N+1)$. We can link the new system ($N+1$ plates) to the previous one (N plates) through the network of fluxes represented in Fig. 3 and the equations below:

$$\begin{aligned} i_1 &= T_\alpha(N)i_0 + R(N)j_1 & i_2 &= T(1)i_1 = Ti_0 \\ j_1 &= R(1)i_1 & j_2 &= R_\alpha(N)i_0 + T(N)j_1 = Ri_0 \\ k_1 &= F_d(N)i_0 + F_u(N)j_1 + R_f(N)l_1 & k_2 &= F_d(1)i_1 + T_f(1)k_1 = F_d(N+1)i_0 \\ l_1 &= F_u(1)i_1 + R_f(1)k_1 & l_2 &= F_u(N)i_0 + F_d(N)j_1 + T_f(N)l_1 \\ & & &= F_u(N)i_0 \end{aligned} \tag{13}$$

where $R_f(N)$ and $T_f(N)$ are the reflectance and the transmittance of a pile of N plates at the emission wavelength λ_{em}. Solving Eq. (13) yields expressions of fluorescence $F_u(N+1)$ and $F_d(N+1)$ for a stack of $N+1$ plates:

$$\begin{aligned} F_u(N+1) = F_u(N) &+ \frac{F_d(N)T_\alpha(N)R_{90}(1)}{1-R_{90}(N)R_{90}(1)} + \frac{F_d(N)T_f(N)R_f(1)}{1-R_f(N)R_f(1)} \\ &+ \frac{T_f(N)T_\alpha(N)(F_u(1) + F_u(N)R_f(1)R_{90}(1))}{(1-R_{90}(N)R_{90}(1))(1-R_f(N)R_f(1))} \end{aligned} \tag{14}$$

$$\begin{aligned} F_d(N+1) = &\frac{F_d(1)T_\alpha(N)}{1-R_{90}(N)R_{90}(1)} + \frac{F_d(N)T_f(1)}{1-R_f(N)R_f(1)} \\ &+ \frac{T_f(1)T_\alpha(N)(F_u(1)R_f(N) + F_u(N)R_{90}(1))}{(1-R_{90}(N)R_{90}(1))(1-R_f(N)R_f(1))}. \end{aligned} \tag{15}$$

Since the upward fluorescence $F_u(1)$ and downward fluorescence $F_d(1)$ of a single layer have been calculated earlier in Eq. (12), it is possible to recursively compute these quantities for 2, 3, ...N layers, with N a positive integer, and then to extend the calculation to a real number by interpolation.

3.3. The fluorescence source model

In Eq. (1), we have introduced the spectral fluorescence yield (SFY) of the elementary layer $\phi(\lambda_{ex}, \lambda_{em})$. In the case of a single fluorophore, it can be written as:

$$\phi(\lambda_{ex}, \lambda_{em}) = \xi(\lambda_{ex})Q\eta(\lambda_{em}) \tag{16}$$

with $\xi(\lambda_{ex})$ the excitation efficiency spectrum, Q the fluorescence quantum yield, and $\eta(\lambda_{em})$ the fluorescence emission spectrum normalized to unity so that $\int_0^\infty \eta(\lambda_{em})d\lambda_{em} = 1$. Details for these three terms are provided below. In photosynthetic systems such as plant leaves, red fluorescence is only produced by chlorophyll a but it is well-known that other pigment–protein complexes are involved in fluorescence emission with different spectral and efficiency characteristics. The chlorophylls associated with the photosystems I (PSI) and II (PSII) are the two main fluorophores of plant leaves (Emerson et al., 1957). Carotenoids also play a crucial role in light absorption and partial energy transfer to chlorophylls (Duysens, 1952). We therefore split the source function in two terms, one for each photosystem, and rewrite Eq. (16) as:

$$\phi(\lambda_{ex}, \lambda_{em}) = \sigma_I \xi_I(\lambda_{ex})Q_I \eta_I(\lambda_{em}) + \sigma_{II} \xi_{II}(\lambda_{ex})Q_{II} \eta_{II}(\lambda_{em}) \tag{17}$$
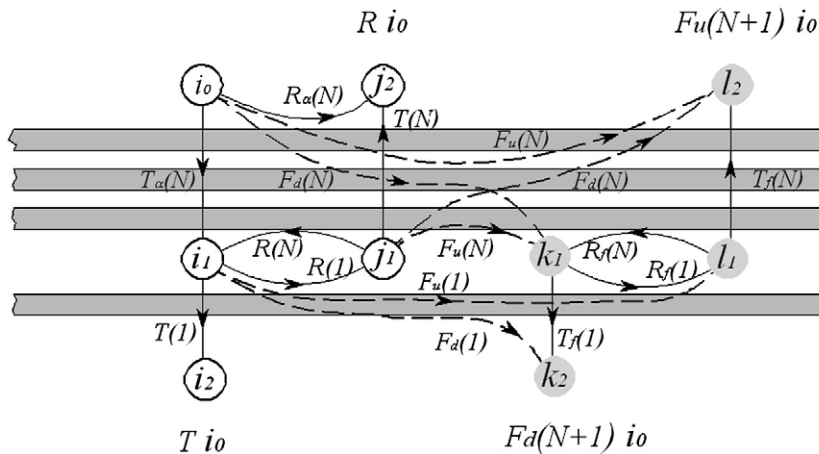

Fig. 3. Flux network of excitation light and fluorescence emission in a pile of $N+1$ plates. i_0, i_1 and i_2 are the downward incident fluxes. j_1 and j_2 are the upward incident fluxes. k_1 and k_2 are the downward fluorescent fluxes. l_1 and l_2 are the upward fluorescent fluxes. Solid line: excitation fluxes, dashed line: emission fluxes.

where the subscripts *I* and *II* stand for photosystems *I* and *II*, respectively. The stoichiometric factors σ_I and σ_{II} satisfying the relation $\sigma_I + \sigma_{II} = 1$ are the relative absorption cross section of PSI and PSII. These constitutive parameters vary with plant species and growth light intensity and quality (Melis & Brown, 1980; Leong & Anderson, 1984).

3.3.1. Excitation efficiency

The excitation efficiency $\xi(\lambda_{ex})$ is the fraction of photons absorbed by or transferred to Chl *a*, among all the absorbed photons that are already quantified in Eq. (2). We introduce this factor at that point because the medium may contain non-fluorescing molecules, or molecules that emit light in another wavelength domain. In plant leaves, this is the case of anthocyanins that absorb light in the blue and the green (Gitelson et al., 2001) or polyphenols that may also produce blue fluorescence when excited by ultraviolet radiation (Cerovic et al., 1999). Carotenoids also belong to this category because they partially transfer their energy to chlorophylls. If we consider an elementary leaf layer illuminated by a collimated beam of light having a uniform flux intensity $I_0(\lambda_{ex})$, its fluorescence is:

$$f(\lambda_{ex}, \lambda_{em}) = I_0(\lambda_{ex}) k(\lambda_{ex})(\sigma_I \eta_I(\lambda_{em}) Q_I \xi_I(\lambda_{ex}) + \sigma_{II} \eta_{II}(\lambda_{em}) Q_{II} \xi_{II}(\lambda_{ex})) \tag{18}$$

with $k(\lambda_{ex})$ the absorption coefficient of PROSPECT. The excitation efficiency of PSI and PSII can be then expressed as:

$$\xi_I(\lambda_{ex}) = \frac{\chi_I(\lambda_{ex})}{k(\lambda_{ex})} \tag{19}$$

$$\xi_{II}(\lambda_{ex}) = \frac{\chi_{II}(\lambda_{ex})}{k(\lambda_{ex})} \tag{20}$$

where $\chi_I(\lambda_{ex})$ and $\chi_{II}(\lambda_{ex})$ are the number of photons absorbed by the fluorescent pigments of photosystems *I* and *II*, respectively. In that case fluorescence is directly related to $\chi_I(\lambda_{ex})$ and $\chi_{II}(\lambda_{ex})$:

$$f(\lambda_{ex}, \lambda_{em}) = I_0(\lambda_{ex})(\sigma_I \chi_I(\lambda_{ex}) Q_I \eta_I(\lambda_{em}) + \sigma_{II} \chi_{II}(\lambda_{ex}) Q_{II} \eta_{II}(\lambda_{em})). \tag{21}$$

We experimentally assessed $\chi_I(\lambda_{ex})$ and $\chi_{II}(\lambda_{ex})$ using dilute solutions of PSI and PSII, which are comparable to an infinitesimal layer because very little scattering occurs in such a medium. By choosing $(\sigma_I, \sigma_{II}) = (1, 0)$ (pure PSI fraction) or $(\sigma_I, \sigma_{II}) = (0, 1)$ (pure PSII fraction), and by varying the excitation wavelength while fixing the emission wavelength at 740 nm where reabsorption is very low, we measured the relative excitation spectra $\chi_I(\lambda_{ex})$ and $\chi_{II}(\lambda_{ex})$. Then we normalized them so that their value near the main absorption peak at 660 nm is at the same level as $k_{ab}(\lambda_{ex})$, the specific absorption coefficient of chlorophyll provided by PROSPECT-5 (Feret et al., 2008).
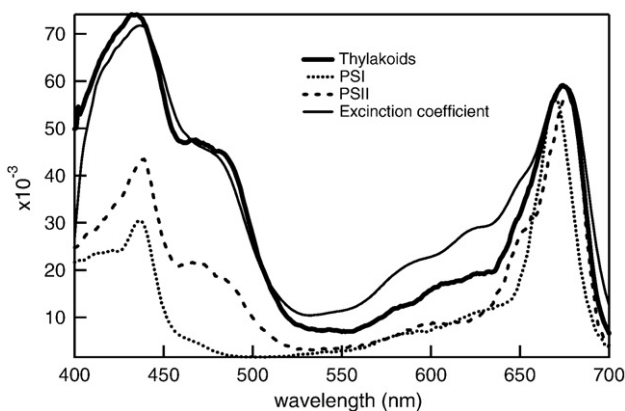
This is justified because chlorophylls *a* and *b* are the only absorbers in this region of the visible spectrum. Fig. 4 shows the normalized excitation spectra of PSI and PSII, compared to the excitation spectrum of entire thylakoids normalized the same way and to $k_{ab}(\lambda_{ex})$. On the one hand, it turns out that the thylakoid spectrum cannot be considered as a combination of measured PSI and PSII excitation spectra, as it was to be expected. Furthermore, the PSI excitation spectrum at 700 nm is generally higher than the PSII excitation spectrum (Franck et al., 2002). These anomalies may be due to conformational changes of the pigment–protein complexes: it is a well-known fact that the extraction procedure modifies the interactions between pigments. Moreover the spectroscopic properties and aggregation state of purified LHC depend on the detergent concentration in the solvent (Bassi et al., 1991; Moya et al., 2001). On the other hand, the thylakoid fluorescence excitation spectrum $\chi_{thy}(\lambda_{ex})$ looks very similar to $k_{ab}(\lambda_{ex})$ as seen in Fig. 4. Therefore, we propose to use it as the excitation spectrum for both photosystems, so that, by combining Eqs. (17) and (20), the source function becomes:

$$\phi(\lambda_{ex}, \lambda_{em}) = \frac{\chi_{thy}(\lambda_{ex})}{k(\lambda_{ex})}(\sigma_I Q_I \eta_I(\lambda_{em}) + \sigma_{II} Q_{II} \eta_{II}(\lambda_{em})). \tag{22}$$

3.3.2. Fluorescence quantum yield

Among all the photons absorbed by Chl *a*, a small fraction *Q* called fluorescence quantum yield is reemitted by fluorescence. Another important parameter is the fluorescence lifetime τ defined as the average time the molecule stays in its excited state before emitting a photon. The quantities *Q* and τ are connected by the relation $Q = \frac{\tau}{\tau_0}$ where τ_0 is the natural fluorescence lifetime of Chl *a* when fluorescence is the only de-excitation pathway. The natural lifetime τ_0 is an intrinsic property of this pigment whether it is involved in PSI or PSII. It is calculated by integration of the absorption curve and is equal to about 15 ns (Brody & Rabinowitch, 1957). The fluorescence lifetime of isolated PSI complexes (τ_I) has long been recognized to be very short: it was found to be about 0.03 ns (Borisov & Il'ina, 1973) and 0.1 ns (Schmuck & Moya, 1994; Agati et al., 2000). Measurements on isolated PSI complexes extracted from *Synechoccocus elongatus* revealed that the PSI fluorescence decay displayed a fast component (13 ps) and a dominant component (~95% of the decay amplitude at the maximum) with lifetimes ranging from 34 ps for open centers to 37 ps for closed centers (Byrdin et al., 2000). This weak variation of τ_I supports the assumption that unlike PSII, PSI fluorescence does not

Fig. 4. Excitation spectra of thylakoids, PSI and PSII suspensions compared to the chlorophyll *a* + *b* specific absorption coefficient of PROSPECT-5 (Feret et al., 2008).
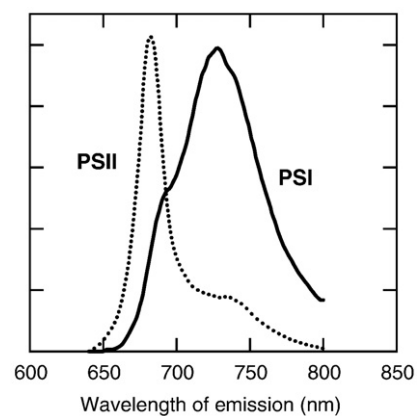

Fig. 5. Normalized elementary emission spectra $\eta(\lambda_{em})$ of isolated PSI (straight line) and PSII (dotted line) in dilute suspension, measured before reabsorption. PSI: PSI-LHCI preparation from maize (*Zea mays*) in a 3 mm × 3 mm cuvette at an optical density of 0.03, excitation wavelength 475 nm, temperature 280 K (Croce et al., 1996). PSII: PSII particles from barley (*Hordeum vulgare*) in a 1 mm cuvette, broad band excitation provided by a white light source filtered with a combination of filters (maximum transmission 446 nm, half-band-width 90 nm) (Franck et al., 2002).

Table 1
Range and standard values of FluorMODleaf input variables.

Variable	Symbol	Range	Standard value	Unit	References
Leaf structure parameter	N	1–2.5	1.5	–	Jacquemoud and Baret (1990)
Chlorophyll $a+b$ content	C_{ab}	0.4–76.8	33.0	µg cm^{-2}	Feret et al. (2008)
Total carotenoid content	C_{cx}	0–25.3	8.0	µg cm^{-2}	Feret et al. (2008)
Water content	C_w	0.0044–0.0340	0.01	cm	Feret et al. (2008)
Dry matter content	C_m	0.0017–0.0331	0.005	g cm^{-2}	Feret et al. (2008)
Relative absorption cross section ratio	σ_{II}/σ_I	1.0–2.4	1.0	–	Anderson and Melis (1983), Yamazaki et al. (1999), Lokstein et al. (2002), Danielsson et al. (2004)
PSI fluorescence lifetime	τ_I	0.034–0.1	0.035	ns	Borisov and Il'ina (1973), Schmuck and Moya (1994), Agati et al. (2000), Byrdin et al. (2000)
PSII fluorescence lifetime	τ_{II}	0.3–2.0	0.5	ns	Schmuck et al. (1991)

change with photochemistry. In the following, we set $\tau_I = 0.035$ ns as a standard value of PSI fluorescence lifetime, although it could be species dependent, which would explain that some authors found higher values. The fluorescence lifetime of PSII (τ_{II}) is much longer than τ_I (Hodges & Moya, 1988), so lifetime measurements on chloroplasts or leaves at 685 nm represent a good approximation of the lifetime of isolated PSII. The PSII quantum yield Q_{II} is known to produce variable chlorophyll fluorescence under the influence of photochemical (closure of the reaction centers) and non-photochemical quenching, and consequently to reflect the physiological state of the plant (for a comprehensive review, see Krause & Weis, 1991). Although several components are involved in the PSII fluorescence emission (Moya et al., 1986), it is long established that the mean fluorescence lifetime t_{II} is almost linearly related to Q_{II} in most experimental conditions (Tumerman & Sorokin, 1967; Moya, 1974). The near-linearity of τ_{II} versus Q_{II} experimentally observed results from energy migration within the photosynthetic antennae pigments.

Thus, the quantum yield Q_{II} can be modeled by the simple relation $Q_{II} = \frac{\tau_{II}}{\tau_0}$ too. Time-resolved fluorescence measurements on leaves showed that τ_{II} varied from 0.3 ns in the F_0 state (Goulas, 1992) to about 2 ns in the F_m state (Schmuck et al., 1991), and that its value was about 0.5 ns in the F_S state (Schmuck et al., 1991). Under natural conditions, the stationary fluorescence F_s stays in the range between F_0 to twice F_0 (Flexas et al., 2000). So we defined the standard conditions for our model by considering lifetimes of 0.035 ns for PSI and 0.5 ns for PSII, which gives:

$$Q_I = \frac{\tau_I}{\tau_0} = \frac{0.035}{15} = 0.23\% \quad \text{and} \quad Q_{II} = \frac{\tau_{II}}{\tau_0} = \frac{0.5}{15} = 3.3\%. \qquad (23)$$

3.3.3. Fluorescence emission spectrum

Fig. 5 shows the native PSI and PSII fluorescence emission spectra that we used in FluorMODleaf (Pedrós et al., 2008). The PSI emission spectrum displays a single broad band at 740 nm (Croce et al., 1996)
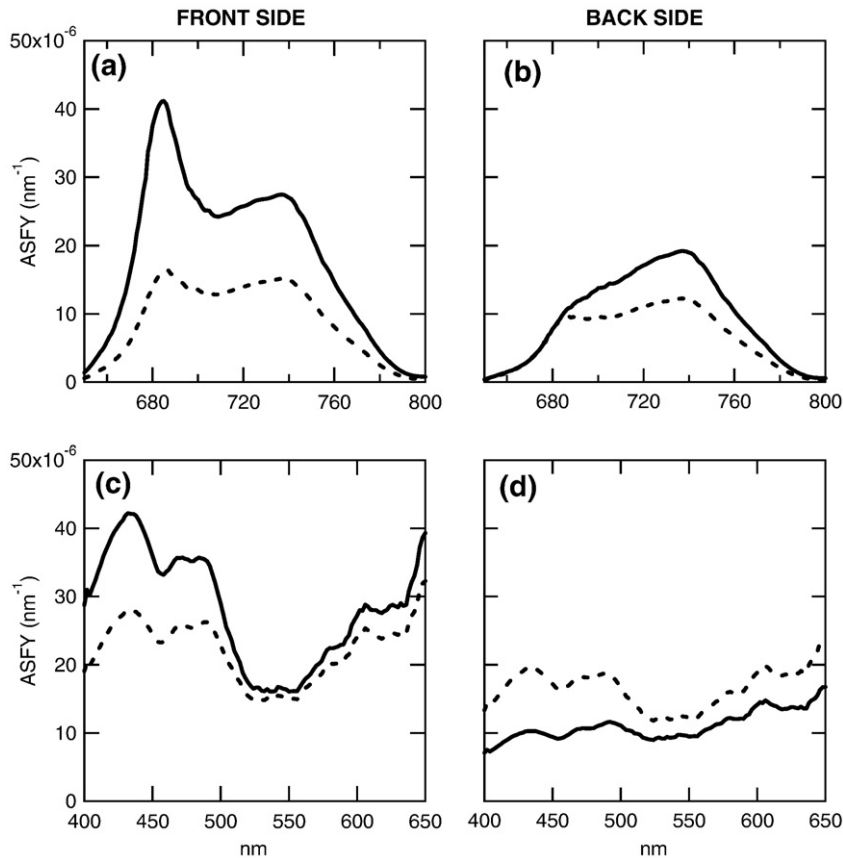

Fig. 6. Apparent spectral fluorescence yield (ASFY) of the standard leaf defined in Table 1. (a–b) Emission spectra at $\lambda_{ex} = 440$ nm (line) and $\lambda_{ex} = 535$ nm (dash); (c–d) Excitation spectra at $\lambda_{em} = 685$ nm (line) and $\lambda_{em} = 735$ nm (dash).

while the main peak of the PSII emission spectrum is at 683 nm, with a shoulder between 700 nm and 750 nm (Franck et al., 2002).

3.3.4. Source function

Combining Eqs. (22) and (23) allows us to write the expression of the source function:

$$\phi(\lambda_{ex}, \lambda_{em}) = \frac{\chi_{thy}(\lambda_{ex})}{\tau_0 k(\lambda_{ex})}(\sigma_I \tau_I \eta_I(\lambda_{em}) + \sigma_{II} \tau_{II} \eta_{II}(\lambda_{em})). \quad (24)$$

4. Model runs and discussion

4.1. Definition of a standard leaf

The eight input variables of FluorMODleaf include the five basic variables of PROSPECT-5 (leaf structure parameter N, chlorophyll $a+b$ content C_{ab}, total carotenoid content C_{cx}, equivalent water thickness C_w and dry matter content C_m) and the three new ones introduced in this paper to control fluorescence emission (σ_{II}/σ_I, τ_I and τ_{II}). We determined the range of variation of each of these input variables on the basis of published data and defined standard values to be used in the following model runs (Table 1). According to Jacquemoud and Baret (1990), the leaf structure parameter N roughly ranges from 1 to 1.5 for monocots, and from 1.5 to 2.5 for dicots, with an average value of $N = 1.5$. The four independent data sets that helped to calibrate and validate PROSPECT-5 (Feret et al., 2008) show consistent statistical distributions for pigments, water and dry matter. Therefore, Table 1 only displays standard values of N, C_{ab}, C_{cx} and C_m extracted from the

ANGERS data set acquired in Angers (France) and containing 276 leaf samples. We determined the standard values of N, C_{ab}, C_{cx}, C_w and C_m as the mean values of these parameters in the ANGERS dataset. The stoichiometric coefficients σ_I and σ_{II} represent the relative absorption cross section of the two photosystems and quantify the relative distribution of light between them. They depend on the concentration of photosystems I and II reaction centers, their distribution in the thylakoids, antenna size and pigment composition, all factors that vary with environmental conditions (Melis, 1989). Plants tend to acclimate to these conditions in order to balance linear electron flow between the two photosystems (Chow et al., 1990). We took the ratio $\sigma_{II}/\sigma_I = 1$ as a standard value for this parameter. If we disregard the effect of pigment composition changes between the two photosystems, σ_{II}/σ_I can be approximated by the product of the PSII/PSI ratio by the antenna size. The range of variation of this product (Table 1) can be retrieved from the literature (Anderson & Melis, 1983; Yamazaki et al., 1999; Lokstein et al., 2002; Danielsson et al., 2004).

4.2. Emission and excitation spectra

We calculated the apparent spectral fluorescence yield (ASFY) of the standard leaf defined in Table 1. Louis et al. (2006) defined it as the ratio of the number of photons emitted by the leaf surface, per unit spectral bandwidth, to the number of incident photons. ASFY is equivalent of the traditional fluorescence emission spectrum expressed as a number of photons but in appropriate units so that its integral over wavelength equals the Apparent Fluorescence Yield (AFY). In this paper, ASFY is expressed in nm^{-1}. Fig. 6a and b displays emission spectra at $\lambda_{ex} = 440$ nm and $\lambda_{ex} = 535$ nm, two excitation wavelengths characteristic of
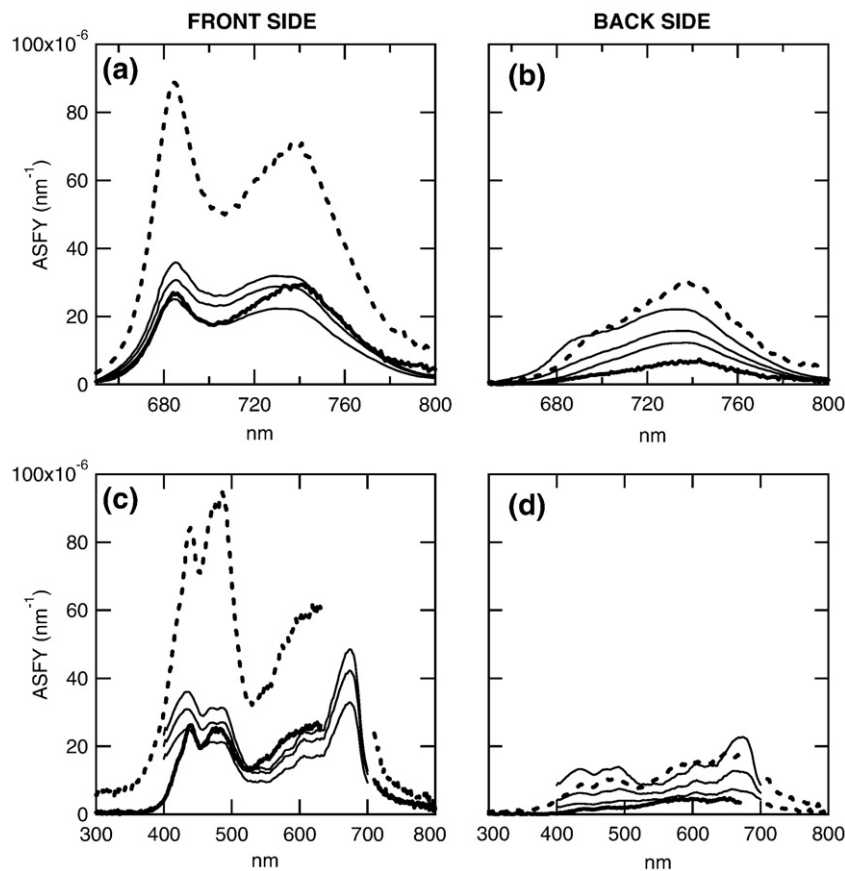

Fig. 7. Apparent spectral fluorescence yield (ASFY) computed by FluorMODleaf compared to measurements acquired on a bean leaf (Louis et al., 2006). Top (a–b): emission spectra at an excitation wavelength of 440 nm. Bottom (c–d): excitation spectra at an emission wavelength of 687 nm. Left (a–c): front-side configuration. Right (b–d): back-side configuration. Thick solid line: the adaxial surface is illuminated. Thick dashed line: the abaxial surface is illuminated. Thin lines: FluorMODleaf simulations with increasing values of the leaf structure parameter N (bottom curve: $N=1$, middle curve: $N=2$, top curve: $N=3$). The other parameters are defined in Table 1, except C_{ab} (24 μg cm^{-2}) and C_{cx} (6 μg cm^{-2}) that are taken in Louis et al. (2006). $\tau_1 = 0.1$ ns and $\tau_{II} = 0.3$ ns (F_0 state).

high and medium pigment absorption regions. Fig. 6c and d displays excitation spectra at $\lambda_{em} = 685$ nm and $\lambda_{em} = 735$ nm, two emission wavelengths aligned with the two main fluorescence emission peaks. These spectra correspond to two different measurement configurations: front-side and back-side that are the situations where fluorescence is measured on the same side and on the opposite side of the light source, respectively. ASFY is about 20 to 40×10^{-6} nm^{-1} in the front-side configuration and 10 to 20×10^{-6} nm^{-1} in the back-side configuration, depending on emission and excitation wavelengths. In the front-side configuration, changing the excitation wavelength from 440 nm to 535 nm induces an overall decrease of ChlF emission and a decrease of the red to far-red fluorescence ratio (RF/FRF) (Fig. 6a). This can be interpreted as a stronger reabsorption of the 535 nm induced fluorescence because green radiation penetrates deeper inside the leaf tissue than blue or red radiation (Vogelmann, 1989), resulting in a longer optical path length (OPL) of fluorescence emission. Switching from front-side to back-side also results in stronger fluorescence reabsorption, as illustrated by the lower overall fluorescence emission and the very low RF/FRF ratio (Fig. 6b).

Very few data have been published on absolute fluorescence yield of leaves. Louis et al. (2006) measured ASFY on dorsiventral bean (*Phaseolus vulgaris* L.) leaves. They found that fluorescence was much higher when the leaves were illuminated on the abaxial side than on the adaxial side, whatever the measurement geometry (Fig. 7). The RF/FRF ratio is also greater on the abaxial side. FluorMODleaf, which assumes that leaves are symmetric, is maybe not the most appropriate tool to simulate the fluorescence of such plant leaves. However, we compared experimental data with FluorMODleaf simulations obtained by varying the input variables to reproduce changes induced by turning the leaf blade upside down. Fig. 7a and c shows that FluorMODleaf reproduces quite well the emission and excitation spectra measured on the adaxial surface in the front-side configuration. However, it fails in simulating the high
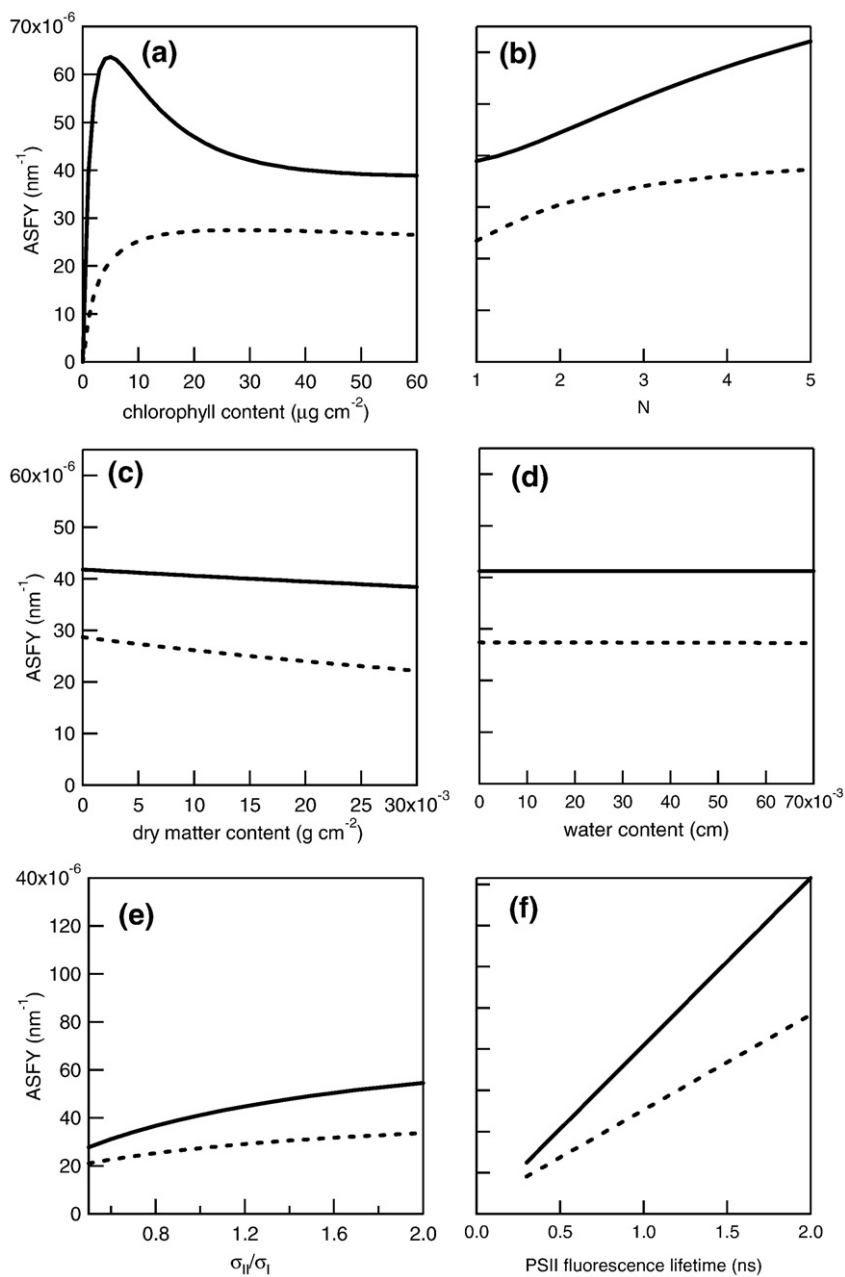

Fig. 8. Fluorescence emission as a function of (a) chlorophyll $a + b$ content, (b) leaf structure parameter, (c) dry matter content, (d) water content, (e) σ_{II}/σ_I ratio, and (f) PSII lifetime τ_{II}. Solid line: emission at 685 nm, dashed line: emission at 735 nm. The other parameters are defined in Table 1.

fluorescence levels observed on the abaxial surface when the leaf structure parameter N varies from 1 to 3 (Fig. 7a and c) or when the other input variables, including Chl content, vary across a physiologically acceptable range (data not shown). This is not the case in the back-side configuration, where an increase of N from 1 to 3 reproduces more accurately the variation of fluorescence observed when shifting from adaxial to abaxial excitation (Fig. 7b and d). The palisade and spongy mesophylls of dicot leaves display very different anatomical structures. For instance, the number of air-cell interfaces is much higher in the spongy mesophyll. Scattering of excitation light and fluorescence is consequently enhanced in this tissue, resulting in increased OPL and greater absorption near the surface. It implies a stronger fluorescence emission with a low reabsorption, as indicated by the higher RF/FRF ratio of the abaxial surface. Indeed, increasing the leaf structure parameter N amounts to shifting from adaxial to abaxial surface, but to a smaller extent. Several hypotheses can be formed to explain the discrepancy between abaxial fluorescence simulated by FluorMODleaf and experimentally measured as in Louis et al. (2006): actual scattering in the spongy mesophyll is much higher than modeled by FluorMODleaf, in particular lateral scattering that may occur to a greater extent; actinic effects change fluorescence when turning the leaf upside down. An improvement of the FluorMODleaf model including leaf asymmetry, as well as complementary measurements, are necessary to better understand side effects in the case of dicot leaves.

4.3. Sensitivity study

Fig. 8 presents variations of fluorescence emission in the front-side configuration, at 685 nm and 735 nm, as a function of six input variables of FluorMODleaf: C_{ab}, N, C_m, C_w, σ_{II}/σ_I and τ_{II}. The largest variation of ChlF is obtained with photosynthetic pigments (Fig. 8a). Fluorescence emissions F685 and F735 steeply increase for low C_{ab} values, but F685 interestingly decreases for $C_{ab} > 5\,\mu g\,cm^{-2}$ while F735 remains almost constant above 20 $\mu g\,cm^{-2}$. At first sight, such a decrease is surprising because one would expect to have more fluorescence when more fluorophore is present. Nevertheless, this effect has already been reported in the literature (Gitelson et al., 1998; Louis, 2004) and is interpreted as an increase of fluorescence reabsorption in the red with increasing chlorophyll content. Additional simulations described hereafter show that scattering plays a major role in the decrease of ChlF with chlorophyll content. Fluorescence emission increases with the leaf structure parameter N both at 685 nm and 735 nm (Fig. 8b). Stacking elementary layers tends to increase multiple scattering and then to lengthen the optical path of light. It could explain the greater absorption of excitation light when N increases and also why fluorescence emission from the abaxial surface is greater than from the adaxial surface (Louis et al., 2006). This was already observed by Virgin (1954) who studied the effect of water infiltration of plant leaves on their fluorescence spectrum. Internal scattering is greatly reduced due to a change in the air volume ratio in the mesophylls. The abaxial part of the mesophyll that contains more intercellular spaces is consequently more diffusive, which can be interpreted by a higher N value. ASFY slightly depends on C_m with a variation of 8% at 685 nm over the range of dry matter content reported in the ANGERS database (Fig. 8c). Water does not absorb visible light so that fluorescence emission does not depend on C_w (Fig. 8d). Finally, fluorescence also increases with σ_{II}/σ_I ratio and τ_{II} (Fig. 8e and f). In both cases, one can notice that the increase in fluorescence is greater at 685 nm than at 735 nm, because the contribution of photosystem II to fluorescence emission is greater in the red than in the far-red. In FluorMODleaf, the quenching state of PSII is represented by τ_{II} which is under the influence of photochemical and non-photochemical quenching. Therefore physiological models should compute the fluorescence quantum yield as a function of environmental parameters and physiological status of the plant, and link it to FluorMODleaf through this parameter.

4.4. Red/far-red fluorescence ratio

It is generally recognized that the RF/FRF ratio decreases when the chlorophyll content increases (for a comprehensive review, see Buschmann, 2007). As the chlorophyll absorption bands overlap the red but not the far-red emission bands, this effect has been attributed to the reabsorption of red light emitted at 685 nm by chlorophyll itself. Fig. 9 illustrates the variation of the ratio F685/F735 with C_{ab}: FluorMODleaf simulations entirely agree with experimental data (Gitelson et al., 1998).

4.5. Effect of scattering on fluorescence emission

Multiple scattering is known to play an important role on light propagation in leaves, and therefore on fluorescence. When modeling fluorescence emission using the KM theory, for instance, it is however difficult to separate absorption from scattering, and extinction coefficients tend to mix these two effects. Some models introduce a factor β that artificially increases the actual extinction coefficient of chlorophyll to account for scattering within the leaf (Agati et al., 1993). In FluorMODleaf, the plate medium itself is supposed to be non-diffusive, so that scattering is only caused by internal reflections at the plate interfaces. It consequently only depends on the refractive index of leaf materials and the number of plates N. We modeled pure scattering effects by varying solely the N parameter (Fig. 8b) and removed them completely by setting all refractive indexes to 1. Variation of ChlF emission as a function of C_{ab} has been computed in the front-side and back-side configurations at two wavelengths: 685 nm where a significant decrease of ChlF is observed in both cases (Fig. 10a) and 735 nm where it is very low (Fig. 10c). When diffusive effects are removed in FluorMODleaf (Fig. 10b and d), the decrease of the front-side ChlF at 685 nm is no longer observed, while ChlF at 735 nm remains almost unchanged. This corresponds to a decrease of fluorescence reabsorption at 685 nm. Indeed, scattering is known to lengthen the optical pathway inside the leaf, thus increasing reabsorption in the red. On the other hand, front-side fluorescence at 685 nm without scattering does not show any decrease with C_{ab} (Fig. 10b) while back-side fluorescence still tends to zero for high chlorophyll contents. This demonstrates that scattering plays a crucial role in the variation of ChlF at 685 nm in the front-side configuration by reflecting part of the fluorescence flux emitted by the deeper layers of the leaf toward the most illuminated ones. (Fig. 10a). Conversely, scattering does not seem to play an important role in the 735 nm emission where reabsorption is low as shown in Fig. 10c and d.
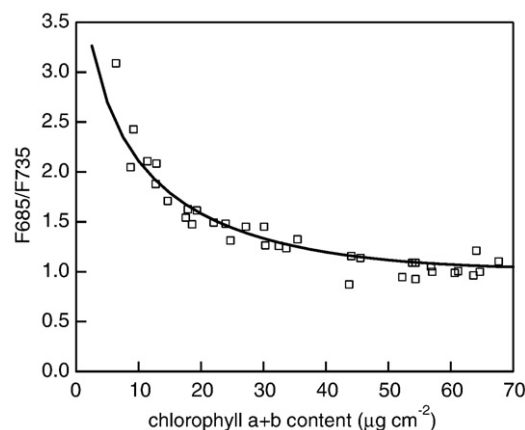

Fig. 9. Red to far-red fluorescence ratio F685/F735 as a function of chlorophyll $a + b$ content for $\lambda_{ex} = 430$ nm. $N = 3$, $\sigma_{II}/\sigma_I = 0.8$ and $\tau_{II} = 0$.ns. The other parameters are defined in Table 1. Solid line: model output. Squares: data taken from Gitelson et al. (1998) and obtained on elm leaves at the same excitation wavelength.
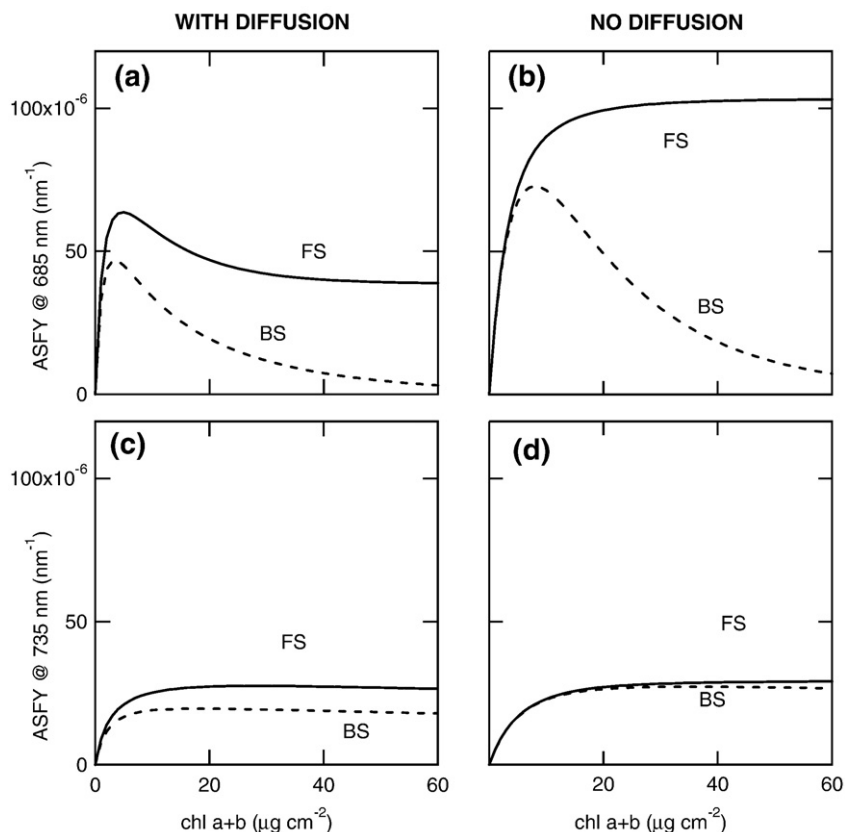
WITH DIFFUSION   **NO DIFFUSION**

Fig. 10. Fluorescence emission as a function of chlorophyll $a + b$ content (a–c) with diffusion and (b–d) without diffusion. Solid line: front-side fluorescence. Dashed lines: back-side fluorescence. (a–b) $\lambda_{em} = 685$ nm and (c–d) $\lambda_{em} = 735$ nm. The other parameters are defined in Table 1.

4.6. Comparison between FluorMODleaf and the Kubelka–Munk theory

Among the others alternative radiative transfer models used to simulate light propagation within plant leaves, the KM theory (Kubelka & Munk, 1931) is the most popular. In this approach, radiation inside a homogeneous medium is modeled by two fluxes traveling in opposite directions and the leaf is characterized by an absorption coefficient k and a scattering coefficient s. At any wavelength λ, the reflectance $R(\lambda)$ and transmittance $T(\lambda)$ can be derived analytically as a function of these two coefficients. An adaptation of the KM theory to fluorescing media has been introduced by Allen (1964), whereas Fukshansky and Kazarinova (1980) and Rosema et al. (1991) extended it to the case of a leaf. Here we use an analytical expression of the first order fluorescence emission, called KMF, derived by integration of the KM propagation equation with Mathematica (Wolfram Research, Inc., Champaign, USA) (see Appendix A). Given a set of input variables for FluorMODleaf, we calculate the leaf reflectance and transmittance at the excitation and emission wavelengths using PROSPECT, and deduce k and s at the same wavelengths by numerical inversion of the KM equations. Then the fluorescence emission computed using KMF is compared to FluorMODleaf outputs for different chlorophyll contents. Fig. 11a and b shows simulations performed at 685 nm and 735 nm in the front-side and back-side configurations. In the KMF model, F685 in the front-side configuration does not decrease with C_{ab}, which contradicts FluorMODleaf
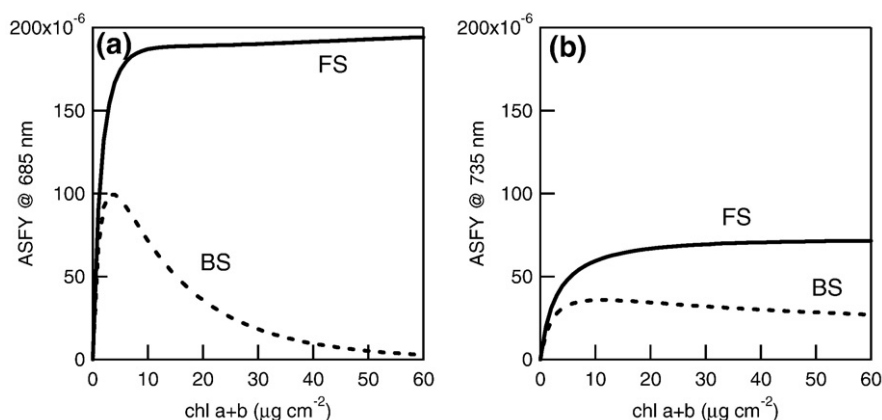

Fig. 11. Fluorescence emission as a function of chlorophyll $a + b$ content in the context of the Kubelka–Munk theory. $\lambda_{ex} = 440$ nm. The other parameters are defined in Table 1. (a) $\lambda_{em} = 685$ nm. (b) $\lambda_{em} = 735$ nm. Solid lines: front-side fluorescence (FS). Dashed lines: back-side fluorescence (BS).

and data previously reported in the literature (Gitelson et al., 1998; Louis, 2004). The comparison between the two models indicates that the coupling between absorption (or reabsorption) and scattering plays an important role in the fluorescence emission of plant leaves. In FluorMODleaf, scattering and absorption occur in separate spatial regions: scattering takes place at the interfaces between the medium and the air, while absorption is limited to the inner medium. On the contrary, in the KMF theory, absorption and scattering are interlinked at every point inside the medium, which results in a different behavior. The comparison between the two approaches suggests that leaf absorption and scattering occur in distinct regions: in chloroplasts where little scattering occurs (absorption) and at the interface between two media separated by different optical indexes (scattering).

5. Conclusion

FluorMODleaf is a new effective chlorophyll *a* fluorescence emission model that simulates the apparent spectral fluorescence yield (ASFY) of a fresh leaf between 640 nm and 840 nm, for any excitation light of the visible spectrum. It is based on PROSPECT, a radiative transfer code that has already proven to generate accurate reflectance and transmittance spectra in the solar domain, and the input variables of which – leaf structure parameter and leaf biochemical content – are well identified. Three new variables have been introduced to drive the emission of light: a stoichiometry factor σ_{II}/σ_I and the two photosystem lifetimes τ_I and τ_{II}. They have a great influence on fluorescence emission but are difficult to assess because the response of the photosynthetic apparatus to them is species dependent and subject to environmental factors such as air temperature, light intensity, etc. For instance, the distribution of air temperature inside a plant canopy which, to some extent, determines the leaf surface temperature is still difficult to measure or model. FluorMODleaf is certainly the first version of a model that will include in the future plant physiology and environmental conditions such as light level, leaf temperature, etc. This means that an additional effort will be necessary to describe the dependency of these variables with respect to the physiological parameters of the species of interest.

The model outputs have been successfully compared to actual measurements for single-wavelength excitations. They reproduce the variations in fluorescence emission spectra associated with chlorophyll content, particularly those caused by a modification in the reabsorption. This work also highlights the importance of scattering that causes spectral deformations that a cursory analysis can easily pass off as something else. Finally, for sunlight excitation (results not shown) the fluorescence levels predicted by the model are consistent with the values published by Kim et al. (1993).

Last but not least, the next step in this ongoing development will consist in coupling FluorMODleaf with FluorSAIL, the counterpart of the SAIL model for fluorescence (Miller et al., 2005), to simulate light emission by a plant canopy. This unique and powerful simulation tool will improve our understanding of vegetation fluorescence for plant status monitoring.

Acknowledgements

Appendix A. Analytical resolution of the Kubelka–Munk equation in the case of a fluorescent medium

The Kubelka–Munk (KM) theory was developed by Kubelka and Munk (1931) to describe the radiative transfer in a painting medium, later found numerous applications in modeling of the optical properties of thin diffuse medium like paper sheets, ink or plant leaves. In the KM theory, radiation within the medium consists of two diffusive fluxes I and J propagating in opposite directions. In the case where there is no fluorescence, I and J can be easily expressed as a linear combination of exponentials function of depth z inside a horizontal slab. Allen (1964) modified the KM equations to include fluorescence. The flow of total diffuse flux across a horizontal slab of thickness dz at any wavelength λ can be written in a differential form as:

$$\begin{cases} \dfrac{dI}{dz} = -(k+s)I + sJ + \dfrac{1}{2}P \\ -\dfrac{dJ}{dz} = sI - (k+s)J + \dfrac{1}{2}P \end{cases} \tag{A1}$$

where s and k are the linear scattering and absorption coefficients for diffuse light (mm^{-1}), I and J are the upward and downward radiant fluxes at depth z, and P is the fluorescence emission flux (assumed to be isotropic) at depth z. By introducing P, we assume that all absorbed photons of I and J in the PAR region contribute to the excitation of the photosystems. P is defined as an integral over the wavelength range 400–700 nm:

$$P(z) = \phi\eta \int_{400}^{700} k(I+J)d\lambda \tag{A2}$$

where ϕ is the photon fluorescence efficiency, i.e., the fraction of absorbed upward and downward fluxes that contributes to fluorescence excitation, and η is the fluorescence emission spectral distribution function. Fukshansky and Kazarinova (1980), Bonham (1986), and Shakespeare and Shakespeare (2003) analytically solved the extended KM equations by successive approximations. Rosema et al. (1991) and later Zarco-Tejada et al. (2000) preferred a numerical procedure called the "doubling method". Finally Emmel (1998, 2000), Emmel and Hersch (1998) proposed a matrix method. Of course, all these methods should provide the same results. Here we proposed a full analytical solution of the extended KM equation in the case of a weakly fluorescent medium, as is ChlF in leaves. In this case, Eq. (A2) can be reformulated as:

$$P(z) = \phi\eta \int_{400}^{700} k(I_0+J_0)d\lambda \tag{A3}$$

where I_0 and J_0 are the upward and downward fluxes when fluorescence is neglected. They can be calculated by solving the KM equations of a non fluorescent medium. The general problem can then be reformulated by considering fluorescence emitted at an emission wavelength λ_2 upon excitation with a monochromatic light at a wavelength λ_1. The set of Eq. (A1) is then rewritten as:

$$\begin{cases} \dfrac{dI(\lambda_1)}{dz} = -(k_1+s_1)I(\lambda_1) + s_1 J(\lambda_1) \\ -\dfrac{dJ(\lambda_1)}{dz} = s_1 I(\lambda_1) - (k_1+s_1)J(\lambda_1) \\ \dfrac{dI(\lambda_2)}{dz} = -(k_2+s_2)I(\lambda_2) + s_2 J(\lambda_2) + \dfrac{1}{2}P(\lambda_1,\lambda_2) \\ -\dfrac{dJ(\lambda_2)}{dz} = s_2 I(\lambda_2) - (k_2+s_2)J(\lambda_2) + \dfrac{1}{2}P(\lambda_1,\lambda_2). \end{cases} \tag{A4}$$

The general solution upon excitation with a polychromatic light can be found by summing solutions obtained with monochromatic light for all wavelengths which make up the polychromatic light. The first two equations of Eq. (A4) are nothing but the KM equations at the excitation wavelength. Their solutions can be expressed analytically in terms of a combination of exponentials depending

on depth z, and reintroduced in the last two equations of Eq. (A4) considering that:

$$P(\lambda_1, \lambda_2) = \phi\eta(\lambda_2)k_1(I(\lambda_1) + J(\lambda_1)). \tag{A5}$$

The last two equations of Eq. (A4) are non homogeneous first order linear differential equations, with a second member which depends exponentially on the variable z, and as such, have solutions in terms of a combination of exponentials. We used Mathematica (Wolfram Research, Inc, Champaign, USA) to compute an analytical expression of the solutions of Eq. (A4). Such solution can be entered into a spreadsheet for calculation of fluorescence emission in the frame of the KM theory. The following mathematical formulae are derived from this solution:

$$\beta_1 = s_1\sqrt{\left(\frac{k_1 + s_1}{s_1}\right)^2 - 1}$$

$$\beta_2 = s_2\sqrt{\left(\frac{k_2 + s_2}{s_2}\right)^2 - 1}$$

$$t_1 = k_1 + 2s_1$$

$$t_2 = k_2 + 2s_2$$

$$u_1 = k_1 + s_1 + \beta_1$$

$$u_2 = k_2 + s_2 + \beta_2$$

$$v_1 = k_1 + s_1 - \beta_1$$

$$v_2 = k_2 + s_2 - \beta_2$$

$$f_1 = 4\beta_1\beta_2(t_2 - t_1)$$

$$f_2 = (t_1 + \beta_1)(\beta_1(\beta_2 + t_2) - t_2(\beta_2 + k_2))$$

$$f_3 = (t_1 + \beta_1)(\beta_1(\beta_2 - t_2) - t_2(\beta_2 - k_2))$$

$$f_4 = (t_1 - \beta_1)(\beta_1(\beta_2 + t_2) + t_2(\beta_2 + k_2))$$

$$f_5 = (t_1 - \beta_1)(\beta_1(\beta_2 - t_2) + t_2(\beta_2 - k_2))$$

$$g_1 = 4\beta_1\beta_2((\beta_2 - t_2)(k_2 + t_1) + 2\beta_2 s_2)$$

$$g_2 = 4\beta_1\beta_2((\beta_2 + t_2)(k_2 + t_1) + 2\beta_2 s_2)$$

$$g_3 = 2(\beta_1 - t_1)(\beta_1 - t_2)(k_2 t_2 + \beta_2^2)$$

$$g_4 = -2(\beta_1 + t_1)(\beta_1 + t_2)(k_2 t_2 + \beta_2^2)$$

$$g_5 = (\beta_1 + t_1)(\beta_1 + t_2)(k_2 t_2 - \beta_2^2)$$

$$g_6 = -(\beta_1 - t_1)(\beta_1 - t_2)(k_2 t_2 - \beta_2^2)$$

$$F_{FS} = \frac{\phi\eta(\lambda_2)k_1}{2(\beta_1 - \beta_2)(\beta_1 + \beta_2)} \frac{f_1 + f_2 e^{\beta_1 + \beta_2} + f_3 e^{\beta_1 - \beta_2} + f_4 e^{-\beta_1 + \beta_2} + f_5 e^{-\beta_1 - \beta_2}}{v_1 v_2 e^{-\beta_1 - \beta_2} - v_1 u_2 e^{-\beta_1 + \beta_2} - u_1 v_2 e^{\beta_1 - \beta_2} + u_1 u_2 e^{\beta_1 + \beta_2}}$$

$$F_{BS} = \frac{\phi\eta(\lambda_2)k_1}{4\beta_2(\beta_1 - \beta_2)(\beta_1 + \beta_2)}$$

$$\frac{g_1 e^{\beta_1 - \beta_2} + g_2 e^{\beta_1 + \beta_2} + g_3 + g_4 e^{2\beta_1} + g_5(e^{2\beta_1 - 2\beta_2} + e^{2\beta_1 + 2\beta_2}) + g_6(e^{2\beta_2} + e^{-2\beta_2})}{-v_1 v_2 e^{-\beta_2} + v_1 u_2 e^{\beta_2} + u_1 v_2 e^{2\beta_1 - \beta_2} - u_1 u_2 e^{2\beta_1 + \beta_2}}. \tag{A6}$$

References

Agati, G., Fusi, F., Mazzinghi, P., & Dipaolo, M. L. (1993). A simple approach to the evaluation of the reabsorption of chlorophyll fluorescence spectra in intact leaves. *Journal of Photochemistry and Photobiology B*, 17, 163−171.

Agati, G., Cerovic, Z., & Moya, I. (2000). The effect of decreasing temperature up to chilling values on the *in vivo* F685/F735 chlorophyll fluorescence ratio in *Phaseolus vulgaris* and *Pisum sativum*: The role of the photosystem I contribution to the 735 nm fluorescence band. *Photochemistry and Photobiology*, 72, 75−84.

Allen, E. (1964). Fluorescent white dyes: Calculation of fluorescence from reflectivity values. *Journal of the Optical Society of America*, 54, 506−515.

Allen, W. A., Gausman, H. W., Richardson, A. J., & Wiegand, C. L. (1970). Mean effective optical constants of thirteen kinds of plant leaves. *Applied Optics*, 9, 2573−2577.

Anderson, J. M., & Melis, A. (1983). Localization of different photosystems in separate regions of chloroplast membranes. *Proceedings of the National Academy of Sciences of the United States of America-Biological Sciences*, 80, 745−749.

Bassi, R., Silvestri, M., Dainese, P., Moya, I., & Giacometti, G. M. (1991). Effects of a nonionic detergent on the spectral properties and aggregation state of the light-harvesting chlorophyll-a/b protein complex (LHCII). *Journal of Photochemistry and Photobiology B-Biology*, 9, 335−354.

Benford, F. (1923). Reflection and transmission by parallel plates. *Journal of the Optical Society of America*, 7, 1017−1025.

Berthold, D. A., Babcock, G. T., & Yocum, C. F. (1981). A highly resolved, oxygen-evolving photosystem II preparation from spinach thylakoid membranes. *FEBS Letter*, 134, 231−234.

Bonham, J. S. (1986). Fluorescence and Kubelka–Munk theory. *Color Research and Application*, 11, 223−230.

Borisov, A. Y., & Il'ina, M. D. (1973). The fluorescence lifetime and energy migration mechanism in photosystem I of plants. *Biochimica et Biophysica Acta*, 305, 364−371.

Brody, S., & Rabinowitch, E. (1957). Excitation lifetime of photosynthetic pigments *in vitro* and *in vivo*. *Science*, 125, 555-555.

Buschmann, C. (2007). Variability and application of the chlorophyll fluorescence emission ratio red/far-red of leaves. *Photosynthesis Research*, 92, 261−271.

Byrdin, M., Rimke, I., Schlodder, E., Stehlik, D., & Roelofs, T. A. (2000). Decay kinetics and quantum yields of fluorescence in photosystem I from *Synechococcus elongatus* with P700 in the reduced and oxidized state: Are the kinetics of excited state decay trap-limited or transfer-limited? *Biophysical Journal*, 79, 992−1007.

Cerovic, Z. G., Samson, G., Morales, F., Tremblay, N., & Moya, I. (1999). Ultraviolet-induced fluorescence for plant monitoring: Present state and prospects. *Agronomie*, 19, 543−578.

Chow, W. S., Melis, A., & Anderson, J. M. (1990). Adjustments of photosystem stoichiometry in chloroplasts improve the quantum efficiency of photosynthesis. *Proceedings of the National Academy of Sciences of the United States of America*, 87, 7502−7506.

Cordon, G. B., & Lagorio, M. G. (2006). Re-absorption of chlorophyll fluorescence in leaves revisited. A comparison of correction models. *Photochemical & Photobiological Sciences*, 5, 735−740.

Cordon, G. B., & Lagorio, M. G. (2007). Absorption and scattering coefficients: A biophysical-chemistry experiment using reflectance spectroscopy. *Journal of Chemical Education*, 84, 1167−1170.

Cordon, G. B., & Lagorio, M. G. (2007). Optical properties of the adaxial and abaxial faces of leaves. Chlorophyll fluorescence, absorption and scattering coefficients. *Photochemical & Photobiological Sciences*, 6, 873−882.

Crilly, R. J., Cheong, W., Wilson, B., & Spears, J. R. (1997). Forward-adjoint fluorescence model: Monte Carlo integration and experimental validation. *Applied Optics*, 36, 6513−6519.

Croce, R., Zucchelli, G., Garlaschi, F. M., Bassi, R., & Jennings, R. C. (1996). Excited state equilibration in the photosystem I-light-harvesting I complex: P700 is almost isoenergetic with its antenna. *Biochemistry*, 35, 8572−8579.

Danielsson, R., Albertsson, P. A., Mamedov, F., & Styring, S. (2004). Quantification of photosystem I and II in different parts of the thylakoid membrane from spinach. *Biochimica et Biophysica Acta — Bioenergetics*, 1608, 53−61.

Davidson, M., Berger, M., Moya, I., Moreno, J., Laurila, T., Stoll, M. P., et al. (2003). Mapping photosynthesis from space — A new vegetation-fluorescence technique. *ESA Bulletin*, 116, 34−37.

Duysens, L. N. M. (1952). Transfer of excitation energy in photosynthesis. PhD Thesis, Utrecht University (Utrecht, The Netherlands).

Emerson, R., Chalmers, R., & Cederstrand, C. (1957). Some factors influencing the long-wave limit of photosynthesis. *Proceedings of the National Academy of Sciences USA*, 43, 133−143.

Emmel, P. (1998). Modèles de prédiction couleur appliqués à l'impression jet d'encre, PhD Thesis, Ecole Polytechnique Fédérale de Lausanne, Lausanne (Suisse), 172 pp.

Emmel, P., & Hersch, R. D. (1998). Spectral colour prediction model for a transparent fluorescent ink on paper. *Proceedings of the 6th Color Imaging Conference: Color Science, Systems and Applications, 17–20 November 1998, Scottsdale (AZ, USA)* (pp. 116−122).

Emmel, P. (2000). Nouvelle formulation du modèle de Kubelka et Munk avec applications aux encres fluorescentes. Actes de l'Ecole de Printemps 2000 - Le pays d'Apt en couleurs, Apt en Roussillon (France).

Feret, J. B., François, C., Asner, G. P., Gitelson, A. A., Martin, R. E., Bidel, L. P. R., et al. (2008). PROSPECT-4 and 5: Advances in the leaf optical properties model separating photosynthetic pigments. *Remote Sensing of Environment*, 112, 3030−3043.

Flexas, J., Briantais, J. M., Cerovic, Z., Medrano, H., & Moya, I. (2000). Steady-state and maximum chlorophyll fluorescence responses to water stress in grapevine leaves: A new remote sensing system. *Remote Sensing of Environment*, 73, 283−297.

Franck, F., Juneau, P., & Popovic, R. (2002). Resolution of the photosystem I and photosystem II contributions to chlorophyll fluorescence of intact leaves at room temperature. *Biochimica et Biophysica Acta*, 1556, 239−246.

Fukshansky, L., & Kazarinova, N. (1980). Extension of the Kubelka–Munk theory of light propagation in intensely scattering materials to fluorescent media. *Journal of the Optical Society of America*, 70, 1101−1111.

Gardner, C. M., Jacques, S. L., & Welch, A. J. (1996). Fluorescence spectroscopy of tissue: Recovery of intrinsic fluorescence from measured fluorescence. *Applied Optics*, 35, 1780−1792.

Georgakoudi, I. (2006). The color of cancer. *Journal of Luminescence*, 119, 75−83.

Gitelson, A. A., Buschmann, C., & Lichtenthaler, H. K. (1998). Leaf chlorophyll fluorescence corrected for re-absorption by means of absorption and reflectance measurements. *Journal of Plant Physiology*, 152, 283−296.

Gitelson, A. A., Merzlyak, M. N., & Chivkunova, O. B. (2001). Optical properties and nondestructive estimation of anthocyanin content in plant leaves. *Photochemistry and Photobiology*, 74, 38−45.

Goulas, Y. (1992). Télédétection de la fluorescence des couverts végétaux: temps de vie de la fluorescence chlorophyllienne et fluorescence bleue. PhD Thesis, Université de Paris-Sud (Orsay, France), 198 pp.

Grace, J., Nichol, C., Disney, M., Lewis, P., Quaife, T., & Bowyer, P. (2007). Can we measure terrestrial photosynthesis from space directly, using spectral reflectance and fluorescence? *Global Change Biology, 13*, 1484−1497.

Guanter, L., Alonso, L., Gómez-Chova, L., Amorós-López, J., Vila, J., & Moreno, J. (2007). Estimation of solar-induced vegetation fluorescence from space measurements. *Geophysical Research Letters, 34*, L08401.

Gupta, S., Raja, V., & Pradhan, A. (2006). Simultaneous extraction of optical transport parameters and intrinsic fluorescence of tissue mimicking model media using a spatially resolved fluorescence technique. *Applied Optics, 45*, 7529−7537.

Hodges, M., & Moya, I. (1988). Time-resolved chlorophyll fluorescence studies on pigment–protein complexes from photosynthetic membranes. *Biochimica and Biophysica Acta, 935*, 41−52.

Jacquemoud, S., & Baret, F. (1990). PROSPECT: A model of leaf optical properties spectra. *Remote Sensing of Environment, 34*, 75−91.

Kim, M. S., Chappelle, E. W., Corp, L., & McMurtrey, J. E., III (1993). The contribution of chlorophyll fluorescence to the reflectance spectra of green vegetation. *Proceedings of the International Geoscience and Remote Sensing Symposium (IGARSS '93), 3*, 1321–1224.

Krause, G. H., & Weis, E. (1991). Chlorophyll fluorescence and photosynthesis: The basics. *Annual Review of Plant Physiology and Plant Molecular Biology, 42*, 313−349.

Kubelka, P., & Munk, F. (1931). Ein Beitrag zur Optik der Farbanstriche. *Zeitschrift für Technische Physik, 12*, 593−601.

Laasch, H. (1987). Non-photochemical quenching of chlorophyll a fluorescence in isolated chloroplasts under conditions of stressed photosynthesis. *Planta, 171*, 220−226.

Leong, T. Y., & Anderson, J. M. (1984). Adaptation of the thylakoid membranes of pea chloroplasts to light intensities. I. Study on the distribution of chlorophyll–protein complexes. *Photosynthesis Research, 5*, 105−115.

Lokstein, H., Tian, L., Polle, J. E. W., & DellaPenna, D. (2002). Xanthophyll biosynthetic mutants of *Arabidopsis thaliana*: Altered nonphotochemical quenching of chlorophyll fluorescence is due to changes in photosystem II antenna size and stability. *Biochimica et Biophysica Acta — Bioenergetics, 1553*, 309−319.

Louis, J. (2004). Télédétection et modélisation des signaux de fluorescence et de réflectance (PRI) des couverts végétaux. PhD Thesis, Université Paris Diderot - Paris 7, Paris (France), 201 pp.

Louis, J., Cerovic, Z. G., & Moya, I. (2006). Quantitative study of fluorescence excitation and emission spectra of bean leaves. *Journal of Photochemistry and Photobiology B, 85*, 65−71.

Maier, S. W. (2000). Modeling the radiative transfer in leaves in the 300 nm to 2.5 μm wavelength region taking into consideration chlorophyll fluorescence − The leaf model SLOPE. PhD Thesis, Technische Universität München, Oberpfaffenhofen (Germany), 110 pp.

Melis, A., & Brown, J. S. (1980). Stoichiometry of system I and system II reaction centers and of plastoquinone in different photosynthetic membranes. *Proceedings of the National Academy of Sciences of the United States of America-Biological Sciences, 77*, 4712−4716.

Melis, A. (1989). Spectroscopic methods in photosynthesis: Photosystem stoichiometry and chlorophyll antenna size. *Philosophical Transactions of the Royal Society of London Series B-Biological Sciences, 323*, 397−409.

Miller, J., Berger, M., Goulas, Y., Jacquemoud, S., Louis, J., Mohammed, G., et al. (2005). Development of a vegetation fluorescence canopy model ESTEC Contract No. 16365/02/NL/FF, (http://www.ias.csic.es/fluormod/documents/FluorMOD_Final_Report_April_13_2005.pdf), 138 pp.

Monteith, J., & Unsworth, M. (2007). *Principles of environmental physics*, Third Edition: Academic Press 440 pp.

Moya, I. (1974). Durée de vie et rendement de fluorescence de la chlorophylle *in vivo*. Leur relation dans différents modèles d'unités photosynthétiques. *Biochimica et Biophysica Acta, 368*, 214−227.

Moya, I., Hodges, M., & Barbet, J. C. (1986). Modification of room-temperature picosecond chlorophyll fluorescence kinetics in green algae by photosystem II trap closure. *FEBS letters, 198*, 256−262.

Moya, I., Guyot, G., & Goulas, Y. (1992). Remotely sensed blue and red fluorescence emission for monitoring vegetation. *ISPRS Journal of Photogrammetry and Remote Sensing, 47*, 205−231.

Moya, I., Silvestri, M., Vallon, O., Cinque, G., & Bassi, R. (2001). Time-resolved fluorescence analysis of the photosystem II antenna proteins in detergent micelles and liposomes. *Biochemistry, 40*, 12552−12561.

Moya, I., & Cerovic, Z. G. (2004). Remote sensing of chlorophyll fluorescence: Instrumentation and analysis. In G. C. Papageorgiou X Govindjee (Eds.), *Chlorophyll a fluorescence: A signature of photosynthesis (pp. 429–445)*. Springer.

Mullet, J. E., Burke, J. J., & Arntzen, C. J. (1980). Chlorophyll proteins of photosystem I. *Plant Physiology, 65*, 814−822.

Ounis, A., Cerovic, Z. G., Briantais, J. M., & Moya, I. (2001). Dual-excitation FLIDAR for the estimation of epidermal UV absorption in leaves and canopies. *Remote Sensing of Environment, 76*, 33−48.

Panou-Diamandi, O., Uzunoglu, N. K., Zacharakis, G., Filippidis, G., Papazoglou, T., & Koutsouris, D. (1998). A one layer tissue fluorescence model based on electromagnetic theory. *Journal of Electromagnetic Waves & Applications, 12*, 1101−1121.

Pedrós, R., Moya, I., Goulas, Y., & Jacquemoud, S. (2008). Chlorophyll fluorescence emission spectrum inside a leaf. *Photochemical & Photobiological Sciences, 7*, 498−502.

Ramos, M. E., & Lagorio, M. G. (2004). True fluorescence spectra of leaves. *Photochemical & Photobiological Sciences, 3*, 1063−1066.

Richards-Kortum, R., Rava, R. P., Fitzmaurice, M., Tong, L. L., Ratliff, N. B., Kramer, J. R., et al. (1989). A one-layer model of laser-induced fluorescence for diagnosis of disease in human tissue: Applications to atherosclerosis. *IEEE Transactions on Bio-Medical Engineering, 36*, 1222−1232.

Rosema, A., Verhoef, W., Schroote, J., & Snel, J. F. H. (1991). Simulating fluorescence light-canopy interaction in support of laser-induced fluorescence measurements. *Remote Sensing of Environment, 37*, 117−130.

Schmuck, G., Verdebout, J., Koechler, C., Moya, I., & Goulas, Y. (1991). Laser-induced time resolved fluorescence of vegetation. *IEEE Transactions on Geoscience and Remote Sensing, 29*, 674−678.

Schmuck, G., & Moya, I. (1994). Time-resolved chlorophyll fluorescence spectra of intact leaves. *Remote Sensing of Environment, 47*, 72−76.

Shakespeare, T., & Shakespeare, J. (2003). A fluorescent extension to the Kubelka–Munk model. *Color Research and Application, 28*, 4−14.

Sušila, P., & Nauš, J. (2007). A Monte Carlo study of the chlorophyll fluorescence emission and its effect on the leaf spectral reflectance and transmittance under various conditions. *Photochemical & Photobiological Sciences, 6*, 894−902.

Tumerman, L. A., & Sorokin, E. M. (1967). The photosynthetic unit: A "physical" or "statistical" model? *Molecular Biology (USSR), 1*, 628−638.

Virgin, H. I. (1954). The distortion of fluorescence spectra in leaves by light scattering and its reduction by infiltration. *Physiologia Plantarum, 7*, 560−570.

Vogelmann, T. C. (1989). Penetration of light into plants. *Photochemistry and Photobiology, 50*, 895−902.

Welch, A. J., Gardner, C., Richards-Kortum, R., Chan, E., Criswell, G., Pfefer, J., et al. (1997). Propagation of fluorescent light. *Lasers in Surgery and Medicine, 21*, 166−178.

Wu, J., Feld, M. S., & Rava, R. P. (1993). An analytical model for extracting intrinsic fluorescence in a turbid media. *Applied Optics, 32*, 3585−3595.

Yamazaki, J., Kamimura, Y., Okada, M., & Sugimura, Y. (1999). Changes in photosynthetic characteristics and photosystem stoichiometries in the lower leaves in rice seedlings. *Plant Science, 148*, 155−163.

Zarco-Tejada, P. J., Miller, J. R., Mohammed, G. H., & Noland, T. L. (2000). Chlorophyll fluorescence effects on vegetation apparent reflectance: I. Leaf-level measurements and model simulation. *Remote Sensing of Environment, 74*, 582−595.